

A preliminary study on numerical simulation of microwave heating process for chemical reaction and discussion of hotspot and thermal runaway phenomenon

ZHAO Xiang^{1†}, HUANG KaMa¹, YAN LiPing¹ & YAO Yuan²

¹ College of Electronics and Information Engineering, Sichuan University, Chengdu 610064, China;

² Chengdu University of Information Technology, Chengdu 610041, China;

The nonlinear process of microwave heating chemical reaction is studied by means of numerical simulation. Especially, the variation of temperature in terms of space and time, as well as the hotspot and thermal runaway phenomena are discussed. Suppose the heated object is a cylinder and the incident electromagnetic (EM) wave is plane wave, the problem turns out to be a coupling calculation of 2D multi-physical fields. The integral equation of EM field is solved using the method of moment (MoM) and the thermal conduction equation is solved using a semi-analysis method. Moreover, a method to determine the equivalent complex permittivity of reactant under the heating is presented in order to perform the calculation. The numerical results for water and a dummy chemical reaction (A) show that the hotspot is a ubiquitous phenomenon in microwave heating process. When the radius of the heated object is small, the highest temperature occurs somewhere inside the object due to the concentration of the EM wave. While the radius increases to a certain degree, the highest temperature occurs somewhere close to the surface due to the skin effect, and the whole high temperature area shows crescent-shaped. That is in accordance with basic physical principles. If the radius is kept the same in the heating process, the hotspot position of water does not change, while that of reaction A with several radius values varies. For either water or A, the thermal runaway phenomenon in which small difference of radius results in large difference of highest temperature, occurs easily when the radius is small. On the contrary, it is not evident when the radius is large. Moreover, it is notable that the highest temperature in water shows oscillating decreasing trend with the increase of radius, but in reaction A almost decreases monotonously. Further study should be performed to determine if this difference is only an occasional occurrence.

numerical simulation, microwave heating, chemical reaction, hotspot phenomenon, thermal runaway

The microwave thermal effects and specific effects have increasing applications in medicine, chemical engineering and so on^[1-4]. However, the nonlinear process of interaction between microwave and chemical reaction has not been sufficiently and deeply understood. Some phenomenon arising from this process, such as “hotspots phenomenon” where temperature non-uniformity in heated object of local small areas having high tempera-

ture increase occurs, and “thermal runaway” where the temperature varies intensely with small changes of geometrical sizes of the heated object, decreases the security and efficiency of microwave energy application and

Received September 7, 2007; accepted December 24, 2008

doi: 10.1007/s11433-009-0081-6

[†]Corresponding author (email: zhaoxiang59@163.com)

Supported by the National Natural Science Foundation of China (Grant Nos. 60801035 and 60531010)

prevents its further development^[5-7]. So far, most of studies on the mechanism, of interaction between microwave and chemical reaction, are only related with the experimental studies of concrete reactions and qualitative theoretical analysis^[8-11]. Accordingly, by means of numerical simulation for microwave heating chemical reaction presented in this paper, we aim to further the understanding of that complex process in order to explore the mechanism of hotspot phenomenon and thermal runaway.

Chemical reactant can be regarded as a complex mixture with time-varied elements. When it interacts with microwave, its equivalent complex permittivity distribution varies with the chemical reaction process, and in reverse, the heating effect of microwave influences the reaction process. Due to the complexity of the microwave heating chemical reaction, there are reports only about numerical simulation researches for equilibrium process of microwave heating ordinary medium, e.g. water at present^[12,13]. In these researches, firstly, the heating process is described through a group of complex nonlinear partial differential equations, including equation of electromagnetic (EM) field, thermal conduction equation, the relation between complex permittivity of the medium and temperature variation and so on, with initial/boundary conditions. Then a Finite-Difference Time-Domain (FDTD) method is used to solve that group of equations to obtain the variation of both temperature field and EM field distribution in terms of heating time. The classical algorithm is described in Figure 1. The nonlinearity of the problem is demonstrated as follows. For one thing, the EM field is dependent on the complex permittivity distribution of heated medium while it is a function of temperature. For another thing, the temperature field is related directly with dissipated EM power which is determined by the EM field and complex permittivity.

The heated object studied in this paper, includes a certain chemical reaction, whose complex permittivity varies not only with temperature, but also with reaction time. And one of the key points is to determine the complex permittivity distribution of the reaction system in some reaction states. To simplify the calculation, the heated object is considered as an infinite cylinder in free space. The method of moment is used to solve integral equation of EM field, so that a big problem caused by the short time step in FDTD solving Maxwell's equations is avoided.

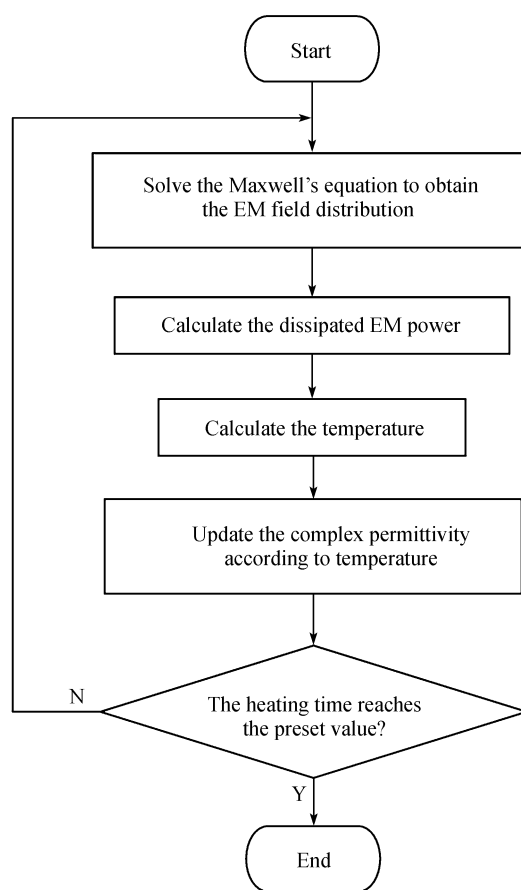


Figure 1 The general algorithm to simulate microwave heating based on FDTD.

1 The calculation model and method

As shown on Figure 2(a), a uniform plane EM wave of angular frequency ω , wavelength $\lambda = 2\pi \frac{3 \times 10^8}{\omega}$ and amplitude E_0 irradiates an infinite cylinder (the heated media), whose complex permittivity is uniformly distributed along the axial direction, that is, \hat{z} direction, so that it is simplified to a 2D problem. Suppose that the circular radius of the cross section S of the heated media is R , and the circle is discretized into many small elements with the same area such as Figure 2(b). And also suppose that each physical quantity is constant in every element. This discrete construction is adopted when both EM field equation and thermal conduction equation are solved.

We use the calculation flow chart of Figure 3 to obtain the process of temperature, EM field and complex permittivity varying with heating time. It can be considered that the growth of temperature is stepping, and EM

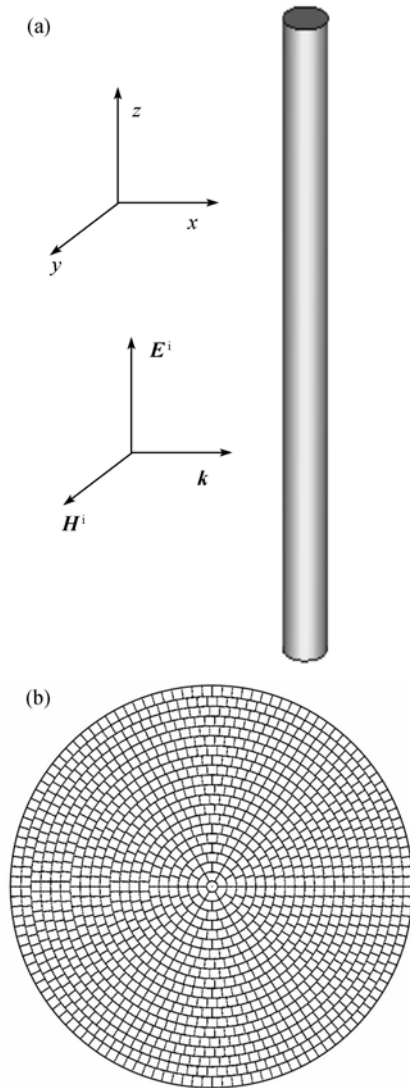


Figure 2 The geometric model and discretized mesh of the problem. (a) Geometric model; (b) discretized mesh.

field distribution reaches a stable state in every step of temperature, attributed to the fact that the growth time of temperature of the heated media is much longer than the period of EM field's variation. As a result, there is no need for EM field equations to be solved in time-domain.

1.1 The method of moment solving the EM field equation

Let us denote complex permittivity of heated media by $\tilde{\epsilon}(\mathbf{r}) = \epsilon'(\mathbf{r}) + j\epsilon''(\mathbf{r})$, here $\mathbf{r} = (r, \varphi)$ is an arbitrary point in S . In terms of Maxwell's equations and time harmonic EM field (time harmonic factor $e^{j\omega t}$), we have the integral equation of electric field intensity $\mathbf{E}(\mathbf{r}) = \hat{z}E(\mathbf{r})$ in S ,

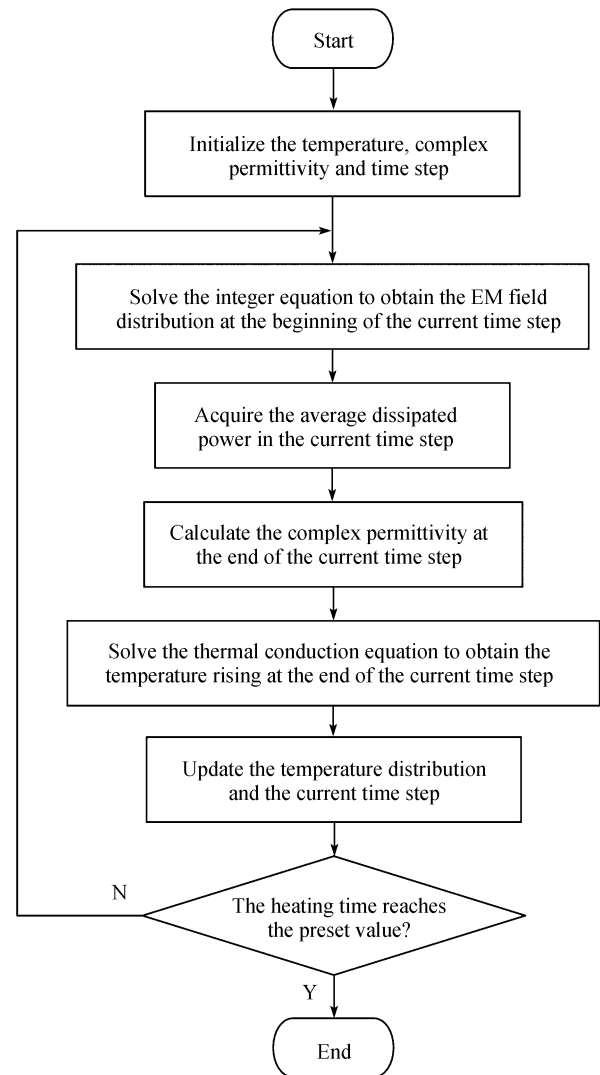


Figure 3 Calculation flow chart used in this paper.

$$\mathbf{E}(\mathbf{r}) = \mathbf{E}^i(\mathbf{r}) + \int_S G(\mathbf{r}, \mathbf{r}') \mathbf{E}(\mathbf{r}') o(\mathbf{r}') dS', \quad (1)$$

where

$$o(\mathbf{r}) = k_0^2 (\tilde{\epsilon}_r(\mathbf{r}) - 1) = k^2(\mathbf{r}) - k_0^2, \quad (2)$$

$$G(\mathbf{r}, \mathbf{r}') = -\frac{j}{4} H_0^{(2)}(k_0 |\mathbf{r} - \mathbf{r}'|). \quad (3)$$

Here, $k_0 = \omega \sqrt{\mu_0 \epsilon_0}$ is the wave number of the background medium, $\tilde{\epsilon}_r(\mathbf{r}) = \tilde{\epsilon}(\mathbf{r}) / \epsilon_0$ the relative complex permittivity, $k(\mathbf{r}) = \omega \sqrt{\mu_0 \tilde{\epsilon}(\mathbf{r})}$, G the two dimensional Green function, $H_0^{(2)}$ is the zero-order Hankel function of the second kind. \mathbf{E} is obtained by using the method of moment to solve eq. (1)^[14]. And the calculated result for a homogeneous circle cylinder is showed in Figure 4, which agrees well with FDTD result in ref. [15].

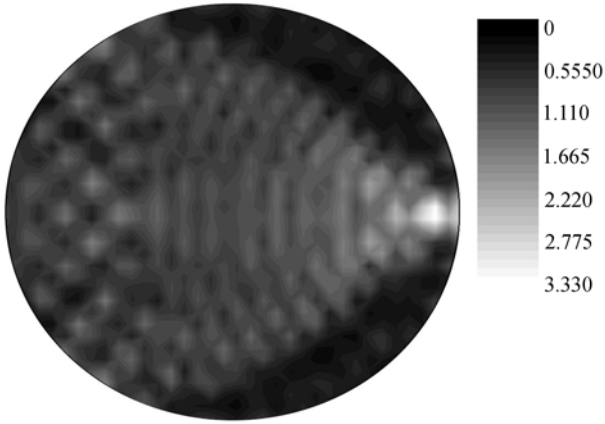


Figure 4 $|E|$ in the homogeneous circle cylinder calculated in this paper ($\varepsilon_r(r) \equiv 3.5$, $R = 2\lambda$, $E_0 = 1$).

1.2 Semi-analytical method solving thermal conduction equation

The infinite cylinder in the EM field is heated attributed to EM polarization and induction. In 2D case, the heating model can be described as thermal conduction equation as follows:

$$K\nabla^2 T(r, \varphi, t) - \rho c \frac{\partial T(r, \varphi, t)}{\partial t} = -F(r, \varphi, t),$$

$$0 \leq r \leq R, \quad -\pi \leq \varphi \leq \pi, \quad t \geq 0. \quad (4)$$

And the initial condition is

$$T(r, \varphi, 0) = T_0, \quad (5)$$

and the boundary condition (thermal insulation) is

$$\left. \frac{\partial T}{\partial n} \right|_{r=R} = 0, \quad (6)$$

where T , K , ρ , c , T_0 and F denote temperature, thermal conductivity, density, specific heat capacity, the initial temperature and the heat source formed by microwave heating, respectively. The thermal convection factor is not taken into account in this model.

Using a differential approximation for the partial derivative of temperature with respect to time:

$$\frac{\partial T(r, \varphi, t)}{\partial t} \approx \frac{T(r, \varphi, t) - T(r, \varphi, t - \Delta t)}{\Delta t}$$

$$= \frac{T(r, \varphi) - T^*(r, \varphi)}{\Delta t} = \frac{\Delta T(r, \varphi)}{\Delta t}, \quad (7)$$

where Δt is the time step, $T(r, \varphi) = T(r, \varphi, t)$ is the temperature at the present time (time t), $T^*(r, \varphi) = T(r, \varphi, t - \Delta t)$ is the temperature at the previous time (time $(t - \Delta t)$), $\Delta T(r, \varphi) = T(r, \varphi) - T^*(r, \varphi)$ is the temperature rising. Then eq. (4) can be written as

$$\nabla^2 (\Delta T(r, \varphi)) - \frac{\rho c}{K \Delta t} \Delta T(r, \varphi) = -\frac{F(r, \varphi)}{K} - \nabla^2 T^*(r, \varphi), \quad (8)$$

where $F(r, \varphi) = \frac{1}{2} \omega \varepsilon_0 \varepsilon'' |E(r, \varphi)|^2$ is the average dissipated power. Let

$$\frac{\rho c}{K \Delta t} = p^2, \quad \frac{F(r, \varphi)}{K} + \frac{\rho c}{K \Delta t} T^*(r, \varphi) = f(r, \varphi).$$

Then, eq. (8) can be written as

$$\nabla^2 (\Delta T(r, \varphi)) - p^2 \Delta T(r, \varphi) = -f(r, \varphi), \quad (9)$$

and the corresponding boundary condition is

$$\left. \frac{\partial \Delta T}{\partial n} \right|_{r=R} = 0. \quad (10)$$

In cylindrical coordinates, eq. (9) can be written as

$$\frac{1}{r} \frac{\partial}{\partial r} \left(r \frac{\partial \Delta T(r, \varphi)}{\partial r} \right) + \frac{1}{r^2} \frac{\partial^2 \Delta T(r, \varphi)}{\partial \varphi^2} - p^2 \Delta T(r, \varphi) = -f(r, \varphi). \quad (11)$$

Let

$$\Delta T(r, \varphi) = \frac{a_0(r)}{2} + \sum_{n=1}^{\infty} [a_n(r) \cos n\varphi + b_n(r) \sin n\varphi], \quad (12)$$

$$f(r, \varphi) = \frac{c_0(r)}{2} + \sum_{n=1}^{\infty} [c_n(r) \cos n\varphi + d_n(r) \sin n\varphi]. \quad (13)$$

Substituting eqs. (12) and (13) into (11) gives

$$a_n''(r) + \frac{a_n'(r)}{r} - \left(\frac{n^2}{r^2} + p^2 \right) a_n(r) = -c_n(r),$$

$$n = 0, 1, 2, \dots, \quad (14)$$

$$b_n''(r) + \frac{b_n'(r)}{r} - \left(\frac{n^2}{r^2} + p^2 \right) b_n(r) = -d_n(r),$$

$$n = 1, 2, \dots. \quad (15)$$

And the corresponding boundary condition is

$$a_n'(R) = b_n'(R) = 0. \quad (16)$$

In order to obtain the solutions $a_n(r)$ ($n = 0, 1, 2, \dots$) and $b_n(r)$ ($n = 1, 2, \dots$) of the inhomogeneous equation above, firstly, it is needed to solve the corresponding homogeneous equation (17) to get the two linearly independent solutions: the N th-order modified Bessel functions $I_n(pr)$ and $K_n(pr)$.

$$\begin{cases} a_n''(r) + \frac{a_n'(r)}{r} - \left(\frac{n^2}{r^2} + p^2 \right) a_n(r) = 0, \\ a_n'(R) = 0. \end{cases} \quad (17)$$

Then, we construct the Green's function of inhomogeneous equations (14) and (15) as follows:

$$G_n(r,s) = \begin{cases} \left(-sK_n(ps) + sI_n(ps) \frac{K'_n(pR)}{I'_n(pR)} \right) I_n(pr), & \text{for } 0 \leq r < s \leq R, \\ sI_n(ps) \frac{K'_n(pR)}{I'_n(pR)} I_n(pr) - sI_n(ps)K_n(pr), & \text{for } 0 \leq s < r \leq R. \end{cases} \quad (18)$$

Thus, the solutions of the inhomogeneous equations (14) and (15) can be obtained by the following equations:

$$a_n(r) = \int_0^R G_n(r,s)c_n(s)ds, \quad n=0, 1, 2, \dots, \quad (19)$$

$$b_n(r) = \int_0^R G_n(r,s)d_n(s)ds, \quad n=1, 2, \dots. \quad (20)$$

In order to verify the Green's function constructed, we deduce the closed-form solution of eqs. (14) and (15), with their boundary condition (16)

$$a_n(r) = Ar^2 \sin nr + r^2 \cos nr, \quad (21)$$

when

$$c_n(r) = -4A \sin nr - 5Anr \cos nr + An^2 r^2 \sin nr - 4 \cos nr + 5nr \sin nr + n^2 r^2 \cos nr + (n^2 (A \sin nr + \cos nr) + p^2 (Ar^2 \sin nr + r^2 \cos nr)),$$

and

$$A = \frac{nR \sin nR - 2 \cos nR}{2 \sin nR + nR \cos nR}. \quad (22)$$

And a comparison between the exact solutions determined by eq. (21) and the calculated ones by the method of Green's function is shown in Figure 5. There is a good agreement between them, which indicates the correctness of this Green's function.

We calculate the case of homogeneous heating in or-

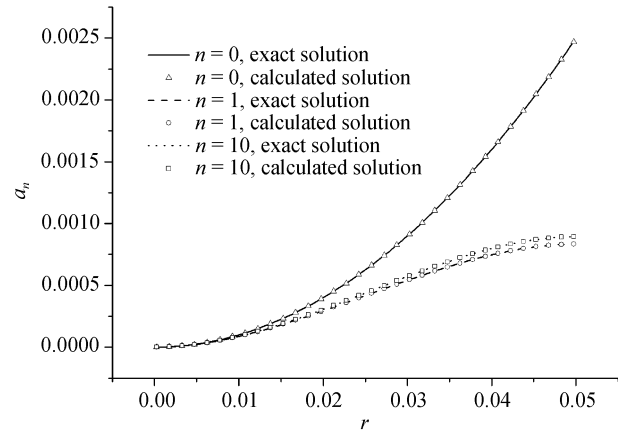


Figure 5 Comparison between exact solutions determined by eq. (21) and calculated ones using the method of Green's function ($p=6055.3$, $R=0.05$).

der to verify the semi-analytical method for solving thermal conduction equation. Assume that the inhomogeneous part in eq. (4) which denotes thermal source is constant F_c , i.e., $F(r, \varphi, t) \equiv F_c$. Then eq. (4) can be simplified as

$$\rho c \frac{\partial T(r, \varphi, t)}{\partial t} = F_c. \quad (23)$$

Combining the initial condition of eq. (5) and the boundary condition of eq. (6), we have

$$T(r, \varphi, t) = F_c \frac{t}{\rho c} + T_0. \quad (24)$$

By eq. (24), it is shown that spatial distribution of temperature is homogeneous and time variation is linear in the case of homogeneous heating. Table 1 shows temperature statistics of spatial variation obtained by the semi-analytical method, and the calculation parameters used are: $\Delta t=0.2$ s, $T_0=300$ K, $c=4180$ J·kg⁻¹·K⁻¹, $\rho=1000$ kg·m⁻³ and $F_c=10^6$. Figure 6 shows the comparison between the average temperatures in Table 1 and the exact solution determined by eq. (24). There is a

Table 1 Temperature statistics of spatial variation obtained by the semi-analytical method in the case of homogeneous heating

Heating time (s)	Average temp. (K)	Lowest temp. (K)	Highest temp. (K)	Variance
0	300	300	300	0
0.2	300.0479	300.0478	300.0479	9.93×10^{-12}
0.4	300.0957	300.0957	300.0957	9.00×10^{-11}
0.6	300.1435	300.1435	300.1435	3.59×10^{-10}
0.8	300.1914	300.1913	300.1914	9.97×10^{-10}
1	300.2392	300.2391	300.2392	2.24×10^{-9}
1.2	300.2871	300.2869	300.2871	4.39×10^{-9}
1.4	300.3349	300.3346	300.3349	7.80×10^{-9}
1.6	300.3827	300.3824	300.3828	1.29×10^{-8}
1.8	300.4306	300.4301	300.4306	2.01×10^{-8}
2	300.4784	300.4779	300.4785	3.01×10^{-8}

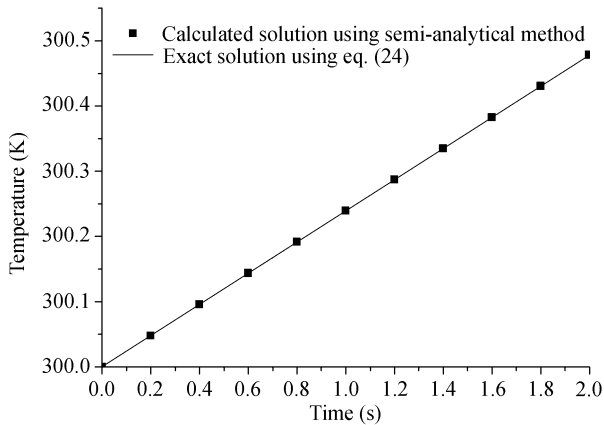


Figure 6 Comparison between the calculated solution using semi-analytical method and the exact solution determined by eq. (24) in the case of homogeneous heating.

good agreement between them, which indicates the correctness of the semi-analytical method.

2 Determination of complex permittivity of the chemical reaction in the heating process

In this section, a method is discussed of how to determine the reactant's (equivalent) complex permittivity distribution in a certain reaction state when heated.

2.1 Determination of complex permittivity at constant temperature

The empirical formula of complex permittivity of the homogeneous chemical reaction in dilute solution is proposed by He et al.^[16] and Hua et al.^[17]:

$$\ln\left(\frac{\varepsilon(T_1, t_1)}{\varepsilon(T_2, t_2)}\right) = -\alpha \ln\left(\frac{T_1}{T_2}\right) - \beta(T_1 - T_2), \quad (25)$$

where $\varepsilon(T, t)$ is the real part or imaginary part of the

complex permittivity when the reaction process is for time t under the temperature T , and $K_1 t_1 = K_2 t_2$ in which K_i is the reaction rate constant corresponding to T_i and α, β are the undetermined coefficients.

As to a concrete chemical reaction, α, β can be determined when the curve of complex permittivity varying with time is measured at several (≥ 3) different temperatures and, furthermore, the complex permittivity variation could be determined at other temperature.

Assume in a chemical reaction, that is called A later, the complex permittivity varying with reaction time is presented in Figure 7, measured at several constant temperature such as 30°C, 37°C and 52°C. According to the method of Huang et al, the variation curve can be determined at some other temperature, 44°C for instance. One of simulation objects in sec. 4 is reaction A .

2.2 Determination of complex permittivity in heating case

Consider the reactant's complex permittivity in one of the sub-regions shown as in Figure 2(b). Let $\tilde{\varepsilon}(T_0, \Delta t)$ be the complex permittivity of the reactant, which has reacted for time Δt at the temperature of T_0 . After being heated for time Δt , the temperature rises to T_1 , and next the reaction continues for time Δt at the temperature of T_1 . Then the complex permittivity denoted by $\tilde{\varepsilon}_{T_0, T_1}$ at this time can be determined by using the following method.

With the idea being the same as in the empirical formula (25), it is believed that, the state of reactant after being in reaction for Δt at T_0 is equivalent to that for time $t_{\text{eff}}^{T_1 \leftarrow T_0}$ at T_1 , where $K_0 \Delta t = K_1 t_{\text{eff}}^{T_1 \leftarrow T_0}$. That is, the

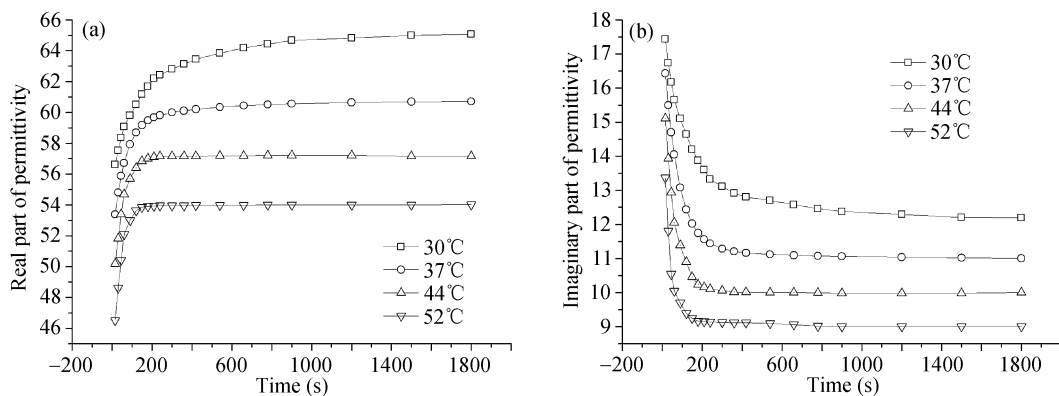


Figure 7 Variation of complex permittivity of reaction A with reaction time at several constant temperatures. (a) Real part; (b) imaginary part.

composition of reactant is the same in both two reaction states, the difference of complex permittivity is only attributed to the difference of temperature. Hence, we have

$$\tilde{\varepsilon}_{T_0, T_1} = \tilde{\varepsilon}(T_1, t_{\text{eff}}^{T_1 \leftarrow T_0} + \Delta t). \quad (26)$$

In other words, $\tilde{\varepsilon}_{T_0, T_1}$ is the complex permittivity when the reaction react time $t_{\text{eff}}^{T_1 \leftarrow T_0} + \Delta t$ starts from the beginning at temperature T_1 .

3 Examples and discussion

The heating process of water and reaction A is calculated in this section. At the frequency of 2.45 GHz, the curves are plotted on Figure 8, which show the complex permittivity of water varying with temperature^[12].

We use these calculation conditions: $E_0 = 2000 \text{ V/m}$, $f = 2.45 \text{ GHz}$, $\Delta t = 0.2 \text{ s}$, $T_0 = 300 \text{ K}$, $K = 0.57 \text{ W} \cdot \text{m}^{-1} \cdot \text{K}^{-1}$, $c = 4180 \text{ J} \cdot \text{kg}^{-1} \cdot \text{K}^{-1}$, $\rho = 1000 \text{ kg} \cdot \text{m}^{-3}$, the total heating time = 200 s, $R = 0.008 - 0.08 \text{ m}$.

Table 2 shows that there exists widely hotspot phenomenon in microwave heating process. No matter for water or reaction A being heated, there are some universal laws. When the radius of the heated object is small, the highest temperature occurs somewhere inside the object due to the concentration of the EM wave. While the radius increases to a certain degree, the highest temperature occurs somewhere close to the surface due to the skin effect, and the whole high temperature area shows crescent-shaped.

Figures 9 and 10 illustrate the water temperature distribution varying with time when the radius R is 0.01 and 0.035 m, and it can be learned that the hotspot position does not change in the water heating process, and the same is true for any other radius. Under the same conditions, the results of reaction A are shown in Figures 11 and 12. The hotspot position in Figure 11 varies obviously, but not in Figure 12. Most of the hotspot positions don't have a change for other radius.

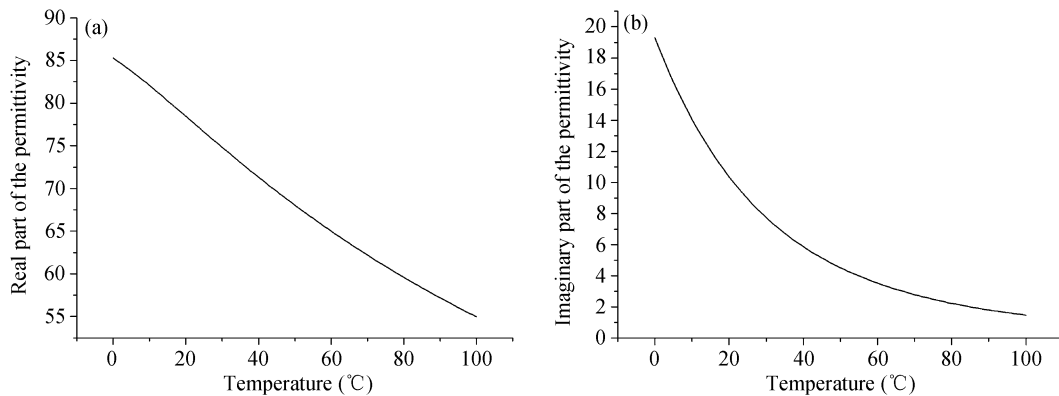


Figure 8 Variation of the complex permittivity of water with temperature at 2.45 GHz. (a) Real part; (b) imaginary part.

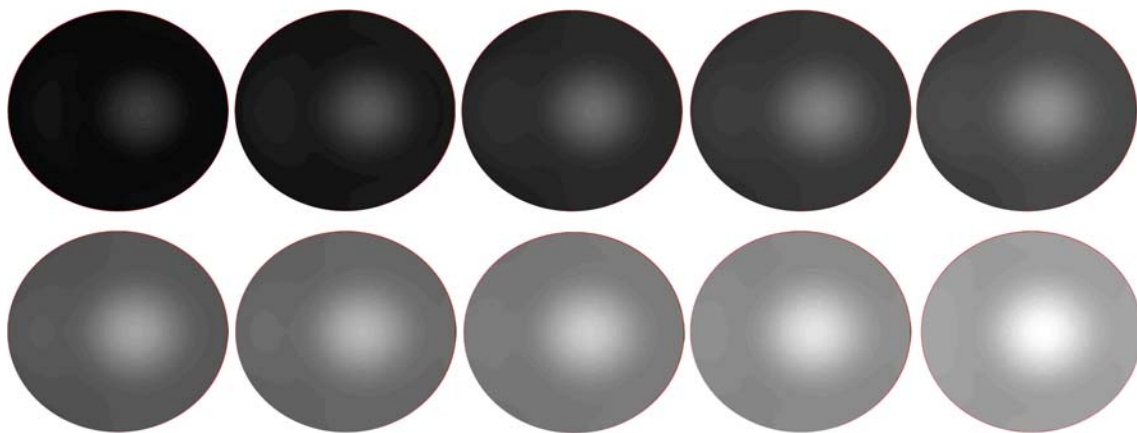
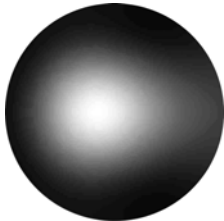
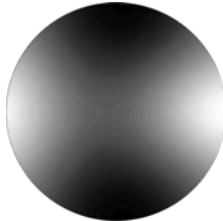
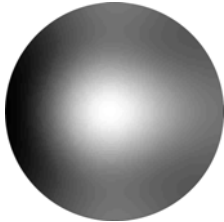
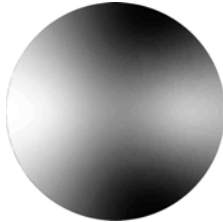
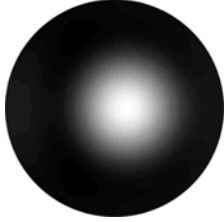
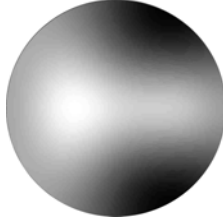
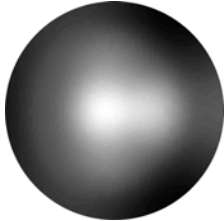
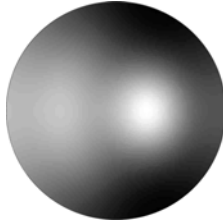
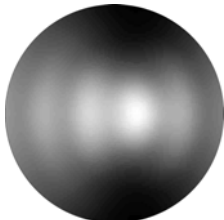
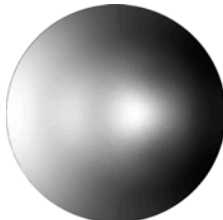
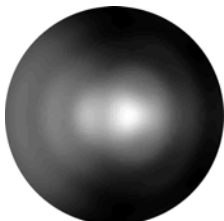
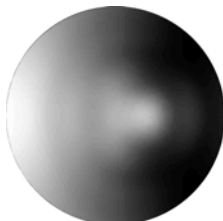
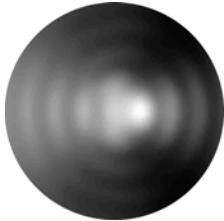
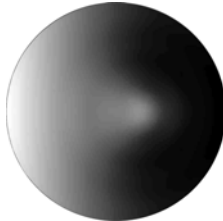
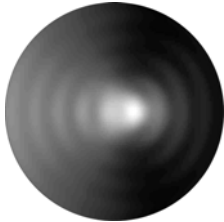
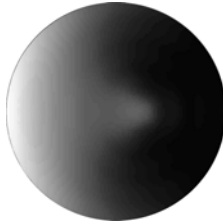
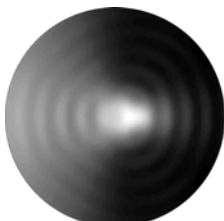
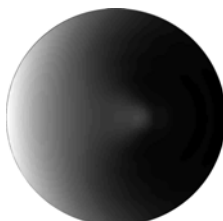
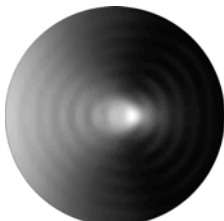
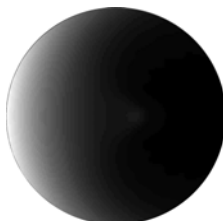
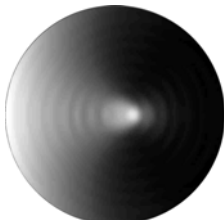





Figure 9 Variation of water temperature distribution with time when $R = 0.01 \text{ m}$ (time interval 20 s).

Table 2 The temperature distribution of water and reactant *A* after being heated for 200 s

<i>R</i> (m)	Water		Reaction <i>A</i>	
	Temp. statistics (K) HT: highest temp. LT: lowest temp. AT: aver. temp.	Temp. distribution graph white: HT black: LT	Temp. statistics (K) HT: highest temp. LT: lowest temp. AT: aver. temp.	Temp. distribution graph white: HT black: LT
0.008	HT: 354.57001 LT: 342.91976 AT: 346.16255		HT: 461.72332 LT: 392.19639 AT: 419.53415	
0.009	HT: 383.16448 LT: 364.64567 AT: 372.96799		HT: 418.94752 LT: 359.7489 AT: 389.26996	
0.01	HT: 366.89135 LT: 340.43139 AT: 345.0005		HT: 412.54075 LT: 364.98162 AT: 390.49252	
0.015	HT: 348.69098 LT: 322.14854 AT: 331.45322		HT: 393.37493 LT: 324.74619 AT: 354.52693	
0.02	HT: 366.97894 LT: 308.47515 AT: 331.79359		HT: 354.52475 LT: 309.20267 AT: 330.82709	
0.025	HT: 343.06342 LT: 308.03215 AT: 317.40016		HT: 351.79673 LT: 303.21694 AT: 323.74274	

(To be continued on the next page)

R (m)	Water		Reaction A	
	Temp. statistics (K) HT: highest temp. LT: lowest temp. AT: aver. temp.	Temp. distribution graph white: HT black: LT	Temp. statistics (K) HT: highest temp. LT: lowest temp. AT: aver. temp.	Temp. distribution graph white: HT black: LT
0.03	HT: 348.28769 LT: 302.76302 AT: 317.15027		HT: 350.62646 LT: 301.28646 AT: 317.95414	
0.035	HT: 338.17901 LT: 301.87464 AT: 311.81138		HT: 348.72663 LT: 300.56182 AT: 314.38182	
0.04	HT: 334.23149 LT: 301.21298 AT: 310.87555		HT: 348.46319 LT: 300.24289 AT: 311.95722	
0.05	HT: 326.3527 LT: 300.37309 AT: 307.72975		HT: 346.32218 LT: 300.0516 AT: 308.76089	
0.06	HT: 319.69233 LT: 300.07538 AT: 305.83965		HT: 343.93722 LT: 300.01299 AT: 306.77451	
0.08	HT: 318.04047 LT: 300.00689 AT: 303.69109		HT: 338.88303 LT: 300.00164 AT: 304.41677	

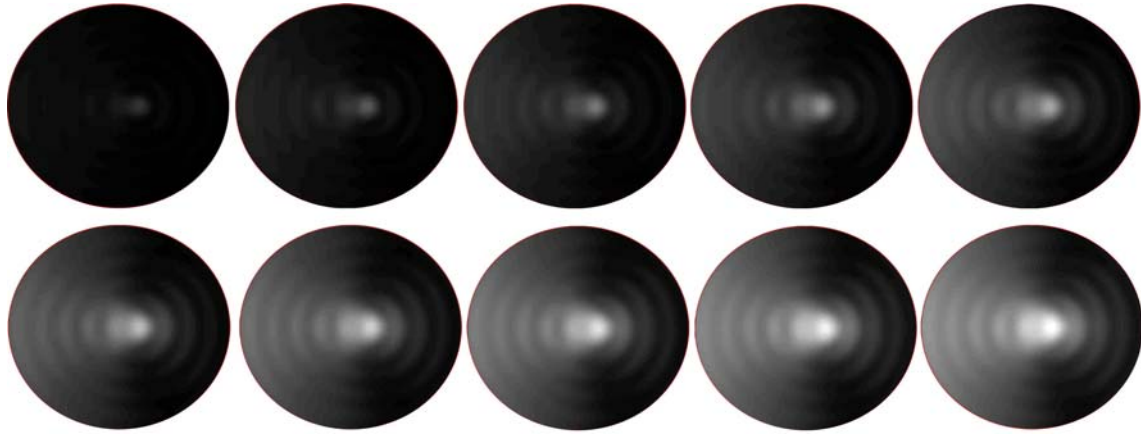


Figure 10 Variation of water temperature distribution with time when $R = 0.035$ m (time interval 20 s).

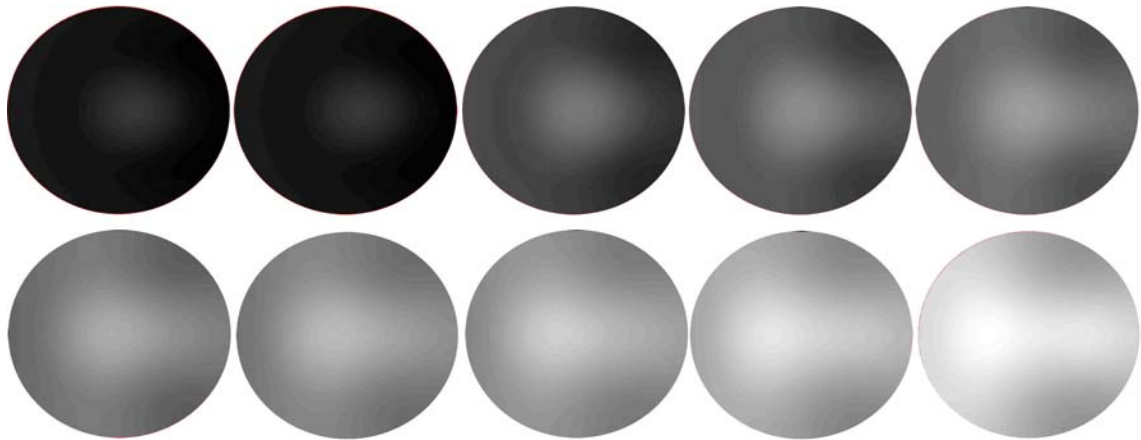


Figure 11 Variation of temperature distribution of reaction A with time when $R = 0.01$ m (time interval 20 s).

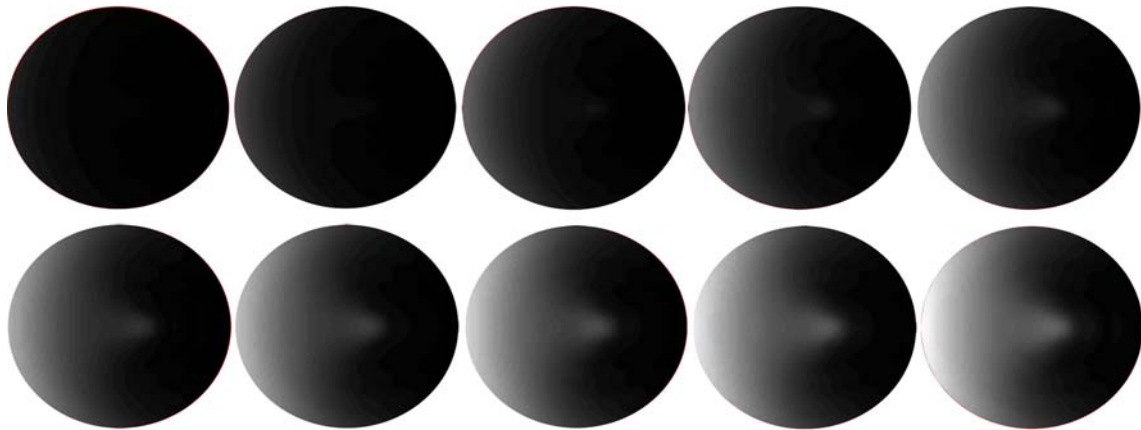


Figure 12 Variation of temperature distribution of reaction A with time when $R = 0.035$ m (time interval 20 s).

It is shown that the highest, lowest and average temperatures vary with radius for the water and reaction A in Figure 13(a) and (b), respectively. It can be found that the highest temperature in water shows oscillating decreasing trend with the increase of radius, but in reaction A almost decreases monotonously. When the radius is

small, the curves rise steeply or drop steeply for both water and reaction A , this is just the thermal runaway phenomenon. On the contrary, when the radius is large, the highest temperatures all drop steadily. In other words, the thermal runaway phenomenon is not evident in this case.

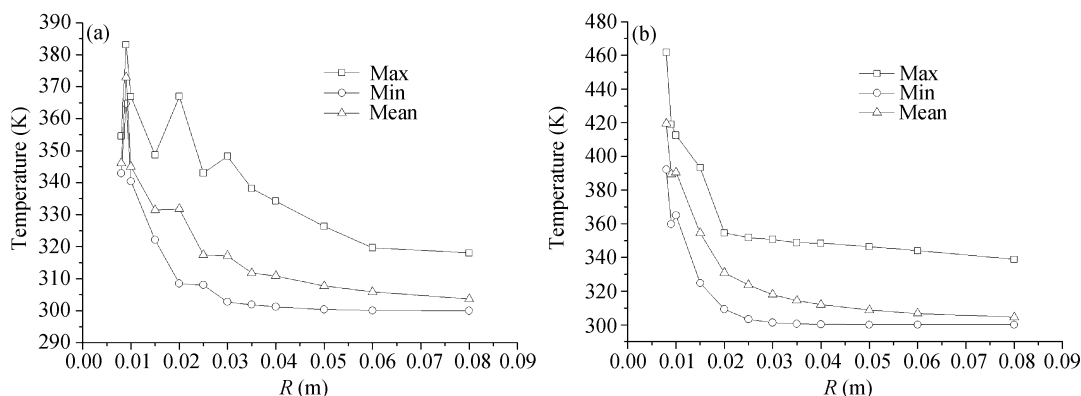


Figure 13 Highest, lowest and average temperature variations with radius. (a) Water; (b) reaction *A*.

4 Conclusion

We present a method of numerical simulation for studying the microwave heating process. In calculation of 2D multi-physical fields, the integral equation of EM field is solved using method of moment (MoM), and the thermal conduction equation is solved using a semi-analysis method. Moreover, a method to determine the equivalent complex permittivity of reactant under the heating is presented in order to perform the calculation. The numerical results for water and a dummy chemical reaction (*A*) show that the hotspot is a ubiquitous phenomenon in microwave heating process. When the radius of the heated object is small, the highest temperature occurs somewhere inside the object due to the concentration of the EM wave. While the radius increases to a certain degree, the highest temperature occurs somewhere close to the surface due to the skin effect, and the whole high temperature area shows crescent-shaped. That is in accordance with basic physical principles. If the radius is kept the same in the heating process, the hotspot position of water does not change, while that of reaction *A* with several radius values varies. For either water or *A*, the thermal runaway phenomenon, in which small difference of radius results in large difference of highest

temperature, occurs easily when the radius is small. On the contrary, it is not evident when the radius is large. Moreover, it is notable that the highest temperature in water shows oscillating decreasing trend with the increase of radius, but in reaction *A* almost decreases monotonously. Further study should be performed to determine if this difference is only an occasional occurrence.

The results presented in this paper are helpful to understand the process of microwave heating general material and chemical reaction, and to control the hotspot and thermal runaway phenomenon to ensure the security and efficiency of the microwave heating process. Another point to mention is that the influence of thermal convection which exists in practice and is highly complex has not been taken into account in the model, which is a general difficulty in numerical simulation for microwave heating process at present. At the same time, the results obtained are needed to compare with the experimental data. However, according to present technique and instrument of temperature measurement, it is a very difficult problem to acquire a relatively accurate result of the temperature distribution in the interior of the medium.

- Jing Q, Dai S, Huang K. Microwave Chemistry. Beijing: Science Press, 1999
- Senise J T, Jermolovicius L A. Microwave chemistry—a fertile field for scientific research and industrial applications. SBMO/IEEE MTT-S International Microwave and Optoelectronics Conference Proceedings, Brazil, 2003. New York: IEEE, 2003. PD01—PD06
- Liang L, Liang Y. The application of microwave radiation technology on organic synthesis. Chemistry, 1996, 26(3): 26—32
- Dayal B, Rao K, Salen G. Microwave-induced organic reactions of bile acids: Esterification, deformylation and deacetylation using mild reagents. J Steroids, 1995, 60(6): 453—457
- Sato M, Roy R, Agrawal D, et al. Microscopic non-equilibrium heating a possible mechanism of microwave effects. International Symposium on Microwave Science and Its Application to Related Fields, Japan, 2004, 339—340
- Roussy G, Mercier J. Temperature runaway of microwave heated materials: Study and control. J Microw Power, 1985, 20(1): 47—51
- Huang K, Yang X. New research of non-thermal effect on the acceleration of chemical reaction with the radiation of microwave. Prog Nat Sci, 2006, 16(3): 273—279

- 8 Stuerger D A C, Gaillard P. Microwave athermal effects in chemistry: A myth's autopsy-part I: Historical background and fundamentals of wave-matter interaction. *J Microw Power Electromagn Energy*, 1996, 31(2): 87–100
- 9 Stuerger D A C, Gaillard P. Microwave athermal effects in chemistry: A myth's autopsy-part II: Orienting effects and thermodynamic consequences of electric field. *J Microw Power Electromagn Energy*, 1996, 31(2): 101–114
- 10 Huang K, Liu Y, Tang J, et al. New characteristics of oxido-reduction reaction of KI and KMnO_4 irradiated by amplitude-modulated electromagnetic waves. *Chin Sci Bull*, 1996, 41(15): 1259–1262
- 11 Huang K, Liu N, Liu C, et al. Preliminary analysis of chemical reaction under the radiation of electromagnetic wave. *Chin Sci Bull*, 2000, 45(19): 1821–1824
- 12 Torres F, Jecko B. Complete FDTD analysis of microwave heating process in frequency-dependent and temperature-dependent media. *IEEE Trans Microw Theory Technol*, 1997, 45(1): 108–116
- 13 Yan L, Huang K, Liu C, et al. Numerical analysis on microwave heating of fluid. *Acta Electron Sin*, 2003, 31(5): 667–670
- 14 Huang K, Zhao X. *Inverse problems and the applications in the electromagnetic field*. Beijing: Science Press, 2005
- 15 Ge D, Yan Y. *The Finite-difference Time-domain Method of Electromagnetic Wave*. Xi'an: Xidian University Press, 2001
- 16 He M, Huang K. The empirical interpolation formula of the equivalent permittivity with temperature for reaction mixture. *Chin J Radio Sci*, 2001, 16(3): 414–417
- 17 Hua W, Yang X. Improved formula to calculate effective permittivity of chemical reaction. *J Chem Ind Eng*, 2006, 57(9): 2111–2115